

## Short duration HF radar echoes observed at mid-latitude during a thunderstorm

### Echos radar de faible durée observés aux latitudes moyennes pendant une période d'activité orageuse

---

A. Bourdillon <sup>(1)</sup>, P. Dorey <sup>(2)</sup> and S. Saillant <sup>(2)</sup>

(1) IETR, Université de Rennes 1, UMR CNRS 6164, Campus de Beaulieu, 35042, Rennes, France, [alain.bourdillon@univ-rennes1.fr](mailto:alain.bourdillon@univ-rennes1.fr)

(2) ONERA, DEMR/RBF, Chemin de la Hunière, 91761 Palaiseau, France

---

**Abstract.** Short duration HF radar ionospheric echoes, lasting from 1 to 5 seconds, have been observed at mid-latitude with the NOSTRADAMUS HF radar. The echoes usually appear in bursts lasting up to 30 seconds with, sometimes, a periodic behaviour. Using beam scanning it was possible to show that most of the reflections occur in the E region, between 90 km and 150 km, and few echoes are observed to come from the D layer between 50 km and 90 km. The processing of short time sequences, with a 0.16 s coherent integration time, shows that the echoing regions are rapidly changing with time and, moreover, they appear in structures aligned along the geomagnetic field lines.

During the observation period, the only noticeable activity was the presence of strong thunderstorms in Western Europe. In the discussion, we propose that lightning-induced electron precipitation (LEP) occurred during the thunderstorm and created localized ionospheric electron density enhancements at the origin of the radar echoes.

**Keywords.** Ionospheric irregularities, HF radar, lightning, whistler, electron precipitation

**Résumé.** Des échos de faible durée, comprise entre 1 et 5 secondes, ont été observés aux moyennes latitudes à l'aide du radar HF NOSTRADAMUS. Ces échos apparaissent dans des paquets dont la durée de vie est de l'ordre de 30 secondes, à l'intérieur desquels le comportement est quasi-périodique. En utilisant les possibilités de balayage de l'espace fournies par l'antenne du radar on montre que ces échos proviennent essentiellement de la région E, entre 90 km et 150 km, mais quelques échos proviennent aussi de la région D entre 50 km et 90 km. Le traitement de séquences courtes (0,16 s) montre des structures plus ou moins alignées le long des lignes de force du champ géomagnétique.

Ces observations ont été faites pendant une période d'intense activité orageuse sur l'Europe de l'Ouest. Dans la discussion on propose que des précipitations d'électrons induites par les éclairs d'orages aient pu créer des irrégularités de la densité électronique à l'origine des échos.

**Mots clés.** Irrégularités ionosphériques, radar HF, éclair, sifflement, précipitation d'électrons

---

### Introduction

Short duration HF radar ionospheric echoes, lasting from 1 to 5 seconds, have been observed at mid-latitude during a scientific campaign performed with the Nostradamus HF radar. For HF radar, the duration of echoes depend on the nature of the target and of the propagation mode. Doppler properties of different propagation modes are described in Table 1. Three propagation modes are considered here: (1) reflection on an ionospheric layer, (2) scattering by irregularities in electron density and (3) reflection on meteor trails. For the echoes considered in this paper, the Doppler shift and width of the spectrum is small and this is consistent with a reflection mode (1) but it is not consistent with a propagation mode involving scattering by ionospheric irregularities.

The short duration echoes presented here appear in bursts lasting up to 30 seconds with, sometimes a more or less periodic behaviour. The Nostradamus radar has the capacity to scan the beam in azimuth and in elevation, offering the possibility to estimate the position (x, y, z) of the reflection point. Most of the reflections occur in the E region between 90 km and 150 km, and few echoes are observed to come also from the D layer between 50 km and 90 km. The processing of short time sequences, with a 0.16 s coherent integration time, shows that the echoing regions change rapidly with time and, moreover, they are organized in structures aligned along the geomagnetic field lines. FFT analysis has been applied to 164 s time sequences, providing a 6 mHz Doppler resolution. The Doppler spectrum of these echoes is very narrow, typically  $\pm 0.5$  Hz (i.e.  $\pm 5.6$  m/s), and it contains several spectral lines spaced by about 50-100 mHz. For each Doppler component, the Doppler shift doesn't vary over several radar gates, typically 50 km or more. While the strongest radar echoes were recorded during the first 40 minutes of the experiment (1800-1840 UT), weaker echoes ( $\sim 20$  dB below) were also observed later in the night.

This event was detected by the HF radar during a quiet period of very low magnetic activity. The only noticeable activity was the presence of a strong thunderstorm in Western Europe. In the discussion, we propose that lightning-induced electron precipitation (LEP) could have occurred during the measurements and created localized ionospheric electron density enhancements at the origin of the radar echoes. This idea is supported by measurements performed at later time on board the DEMETER satellite and showing enhanced whistler activity with associated electron density fluctuations.

Propagation mode	Doppler shift	Doppler width
One hop reflection	small	small
Bragg scattering	large	large
Reflection by meteor trail	large	small

Table 1. General properties of HF radar propagation modes

In the present paper, we present the short duration echoes considered here. The radar observations and the data processing are described in section 1. Section 2 is devoted to the results of the Doppler analysis. The last section is concerned with the discussion and the conclusion.

## 1. Radar data and processing

### 1.1 Radar data

The observations presented here have been performed at mid-latitude using the Nostradamus HF radar located 100 km West of Paris. Figure 1 presents a range-time-intensity (RTI) plot with the short duration echoes that are considered here. The power of radar echoes varies on a time scale of a few seconds up to ten seconds, for the range gates situated between 400 km and 500 km. The coherent integration time (CIT) used here is 0.32 s and the horizontal scale corresponds to 164 seconds. Variations of the power can be as large as 15-20 dB in a few seconds. Figure 1 shows that some periodicities exist in the data and there is a tendency for the echoes to appear in bursts lasting 10-40 seconds. During the experiment, beaming of the radar was  $357^\circ$  for the azimuth (geomagnetic North direction) and  $23^\circ$  for the elevation. For this azimuth and ground ranging of 400-450 km, the reflection point is over the Channel, between France and UK, approximately at about  $50.6^\circ$  N,  $0.9^\circ$  E. The radar experiment started at 18 UT on 19 July 2006 with a 13.4 MHz transmitted frequency, a 10 ms period repetition interval and a FMCW pulsed waveform providing a 5 km range resolution. The signal at the output of the 18 receivers connected to the sub-arrays was recorded after Hilbert filtering in 113 range gates covering a maximum range of 655 km.

The antenna of the radar comprises 3 arms arranged in 18 sub-arrays and each sub-array comprises 16 antennas. Only the central antennas are connected to the transmitters. As a consequence, the transmitting beam is wider than the receiving one. Through antenna phasing and beam forming, beaming of the radar was set at  $357^\circ$  for azimuth and  $23^\circ$  for elevation. For the experimental conditions used here, the 3 dB receiving beam width is  $1.9^\circ$  in azimuth and  $4.6^\circ$  in elevation. Since the transmitting beam is wider than the receiving one, it is possible to compute several receiving beams inside the region illuminated by the transmitting antennas. We have developed

a method, based on beam scanning, to estimate the 3D position (x, y, z) of the echoing region. Most of the time, the fast varying echoes considered here come from the E layer (90-150 km) but sometimes they are also observed to come from the D layer (50-90 km).

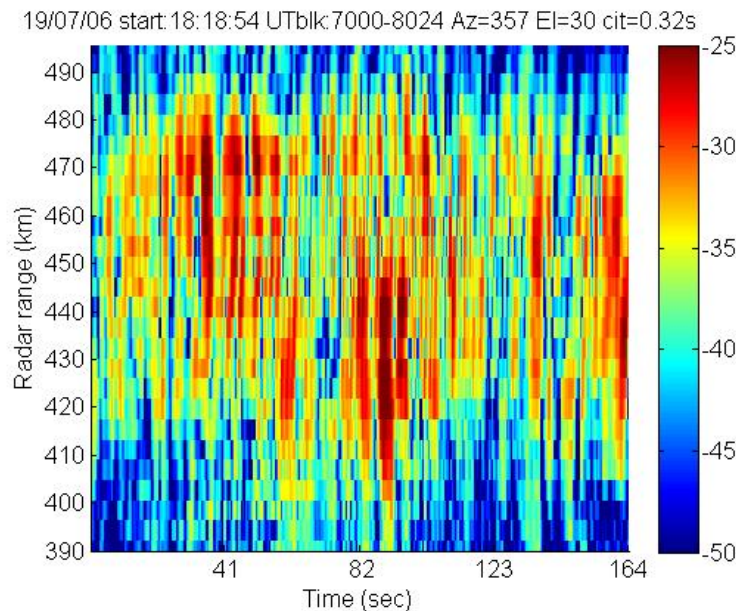


Fig.1 Range-Time-Intensity plot of a sequence starting at 18:18:54 UT on 19 July 2006, for the gates located in range between 390 km and 500 km. Beaming of the radar is  $30^\circ$  in elevation and  $357^\circ$  in azimuth and the duration of the sequence presented is 164 seconds. The coherent integration time is 0.32 s. Strong echoes are observed to vary quickly on a time scale of a few seconds and they appear as bursts of 10-40 s duration. The first burst is observed between 440-480 km starting at to + 20 s while another burst starts at to + 80 s for ranges between 400-450 km (to is the time at the origin of the plot).

## 1.2 Data processing

The complex signal at the output of the 18 receivers is recorded; it is thus possible to process the data off-line and to produce several receiving beams inside the region illuminated by the transmitting beam. The radiation pattern of the antenna array has several ambiguity lobes and it's necessary to take them into account to get the correct position of the targets. The main reason of the existence of ambiguity lobes is that the antenna aperture is partially empty since it is not fully covered with antennas. As a consequence we have to define a processing adapted to the antenna array structure. The processing used here consists in computing several beams, with a small increment in the elevation and azimuth angles, and, for each resolution cell in range, only the beam with the strongest echo is selected and stored in memory. In this way, contamination by ambiguity lobes is minimized. The main drawback of this processing is that weak echoes are also removed from the result since only the beam with the strongest echo is selected by the algorithm. We take advantage of the fluctuations with time of the echo power by plotting several consecutive sequences in the same figure. The spreading of the points gives information on the evolution of the echoing region during the time period covered by the plot.

## 1.3 Scanning in elevation and azimuth

The processing discussed in the previous section allows the production of height-range-intensity (HRI) plots, as shown in figure 2. Sixty one receiving beams were computed in the elevation plane and twenty one beams were computed in azimuth with a  $0.5^\circ$  angular increment (same increment in elevation and in azimuth). Among the 1891 computed beams, the algorithm selects only one beam per resolution cell. The computed beams cover  $\pm 15^\circ$  around the central elevation of the beam ( $30^\circ$ ) and  $\pm 5^\circ$  around the central azimuth ( $357^\circ$ ). Moreover, thirty one time series, each corresponding to a 0.16 s CIT, have been processed sequentially. One example of the results provided by the algorithm is presented in figure 2. For a given range, the beam selected by the algorithm can be different for each CIT. Consequently, the heights and the ground ranges vary, resulting in the spreading of the points when all the sequences are superimposed. The spreading of the points gives information on the spatial extent of the echoing region during the 5 s duration of the sequence processed. To produce figure 2, elevation angle and radar range were used to compute altitude and ground range in spherical geometry. The echo power

was plotted on a colour scale with a 20 dB dynamic range. The propagation mode was assumed to involve a reflection on a plasma layer.

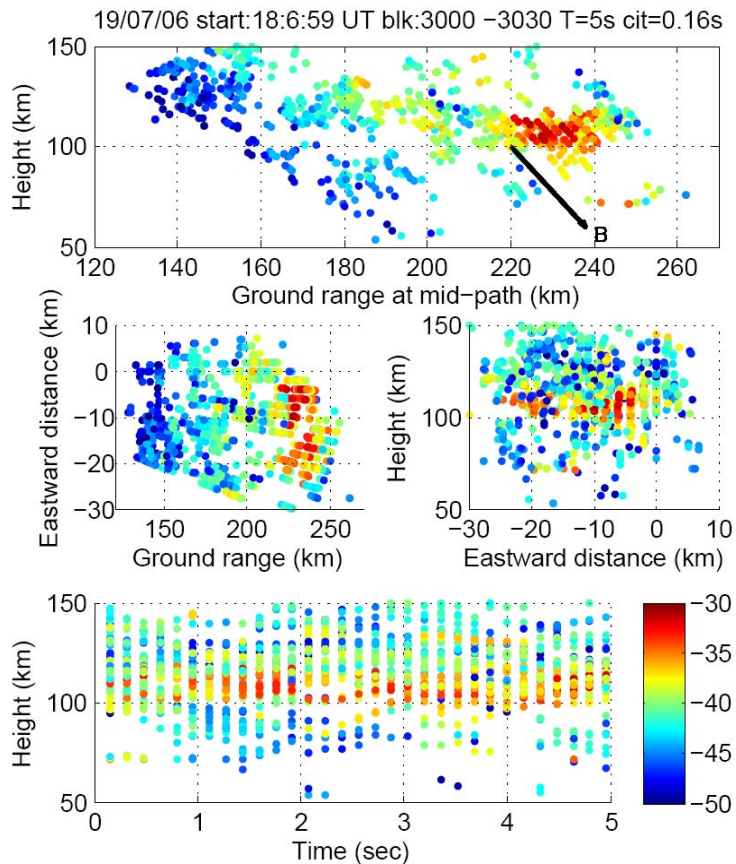


Fig 2. Localization of the radar echoes on 19 July 2006 at 18:06:59 UT. The strongest echoes are observed between altitudes 90 km and 120 km. Upper plot: height versus ground range (at mid-path). The arrow indicates the direction of the magnetic field.

#### 1.4 Results

Figure 2 comprises 4 plots; each of them corresponds to the same time series 5 seconds duration with different projection. The upper plot presents height versus ground range. Here the points are plotted whatever the azimuth. The arrow drawn in figure 2 shows the direction of the Earth magnetic field. The magnetic field inclination was obtained from the IGRF 95 model. The strongest echoes are coming mostly from altitudes higher than 90 km (E layer) and a smallest number of echoes are also coming from altitudes between 50 km and 90 km. This plot shows structures in the echoing region more or less in line with the geomagnetic field. This behaviour was observed on a large part of the processed data. In the middle of figure 2, the panel has two plots: the plot on the left presents a projection on the ground, eastward distance versus ground range (the eastward distance being relative to azimuth zero) and the right panel presents the height versus the eastward distance. The strongest echoes come from 2 regions separated in the EW direction by about 10 km. The lower plot presents the variations of the height of the echoes versus time. The situation is variable with time but the strongest echoes between 100 km and 120 km are observed to last about 5 seconds.

## 2. Doppler processing

The Doppler analysis was performed with a 1024 points Fast Fourier Transform of a 164 s duration time series, providing a 6 mHz resolution. The Doppler spectrum covers  $\pm 3.125$  Hz (figure 3). The spectrum comprises several narrow spectral lines at discrete frequencies in the interval  $\pm 0.5$  Hz (i.e.  $\pm 5.6$  m/s). For the negative shifts and gates ranging from 400 to 460 km, there are two components, separated by about 125 mHz. The positive

(negative) Doppler shifts correspond to a velocity toward (away) from the radar. Figure 4 shows the Doppler spectrum of the sequence recorded 12 minutes after figure 3.

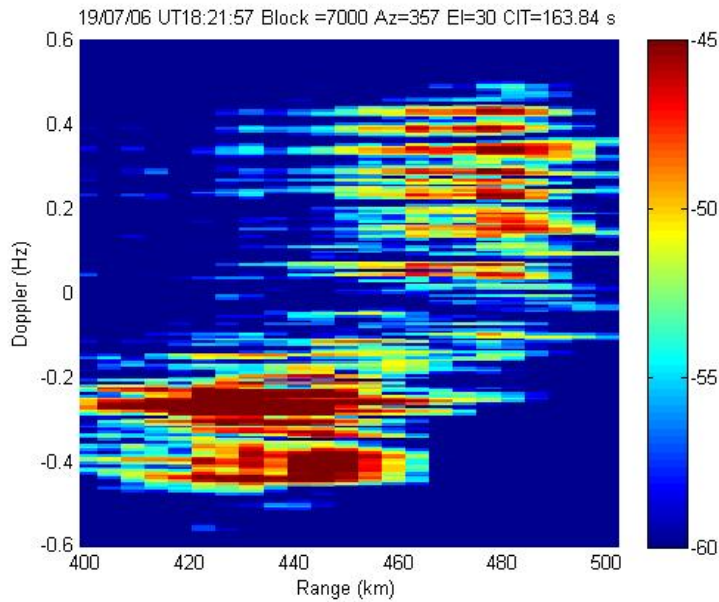


Fig 3. Doppler spectrum of a sequence 163 s duration. The theoretical Doppler resolution is  $\sim 6\text{mHz}$ . The spectrum lies between  $\pm 0.5\text{ Hz}$  (i.e.  $\pm 5.6\text{ m/s}$ ). Negative (positive) Doppler shifts are observed for the nearest (farthest) range gates. The Doppler spectrum comprises lines at discrete frequencies (see next figure).

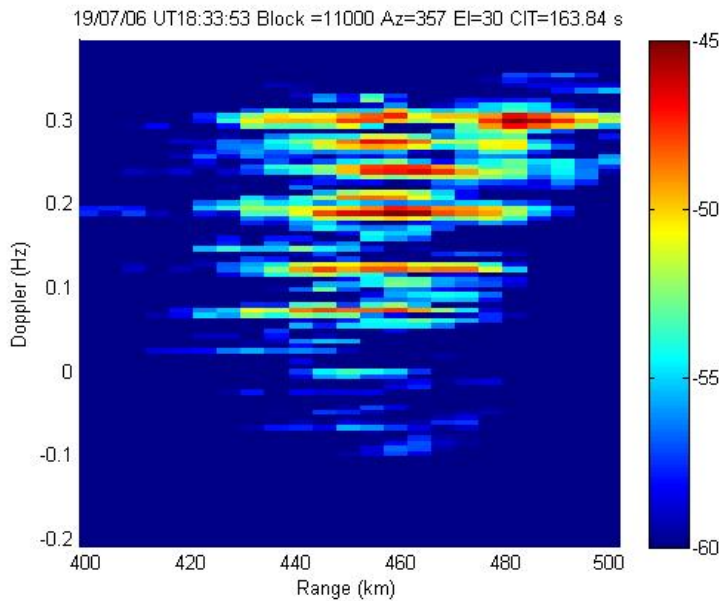


Fig. 4. Doppler spectrum of a sequence 163 s duration, taken 12 minutes after figure 3. The Doppler spectrum shows spectral lines at discrete frequencies on the positive side between 0-0.4 Hz.

Once again the Doppler spectrum shows spectral lines at discrete frequencies on the positive side between 0-0.4 Hz. These properties of the Doppler spectrum are unusual for HF radar echoes. If the echoes were due to backscattering by ionospheric irregularities the spectrum would have been much wider. This is the reason we conclude that propagation involved a reflection on a ionospheric layer or a electron density patch.

### 3. Discussion and conclusion

The characteristics of the fast varying HF radar echoes presented here are very unusual and we have no obvious explanation to propose. The period of observation was very quiet from the magnetic point of view and the only unusual activity was strong thunderstorms occurring over Western Europe. Figure 5 presents a plot of the

lightning observed by the Meteorage system in the interval 18-19 UT. In this figure the radar location is indicated by 'o' and the ionospheric region at the origin of the echoes is shown by the sign '\*'. Three lightning's zones were detected during this period, forming the elongated bands observed in figure 5. In particular, south of the radar, there is a lightning region approximately on the same meridian.

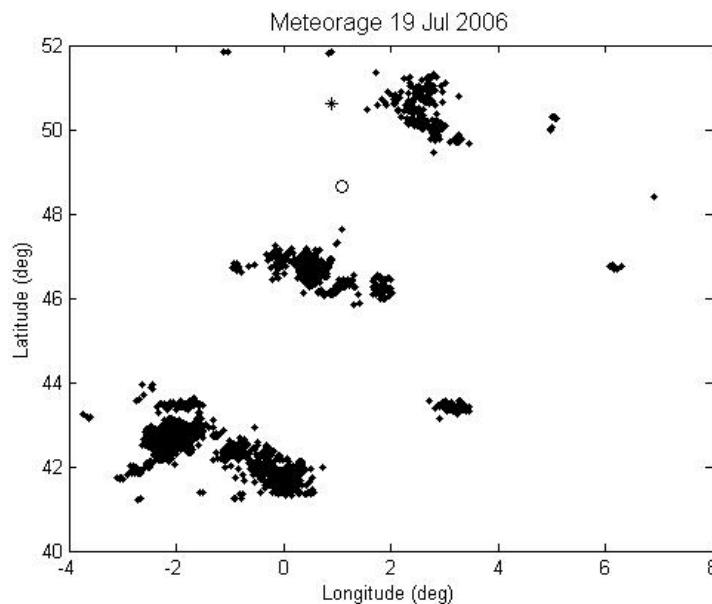


Fig. 5. Map showing the position of the lightning observed by Meteorage in the time interval 18-19 UT. The radar location is indicated by 'o' and the ionospheric region at the origin of the echoes is shown by the sign '\*'. Three lightning zone were detected during this period, forming the elongated bands observed in this figure. South of the radar, there is a lightning region approximately on the same meridian

Short duration echoes have already been observed at low HF frequencies by Roussel-Dupré and Blanc in Africa [1]. In their observations the total duration of the events was about 10 s which is much smaller than the duration of the event presented here. Roussel-Dupré and Blanc have explained their observations by the reflection of HF waves on the column of plasma located above the cloud where the lightning occurred. The event reported in the present paper lasts more than 40 minutes and the echoes come mainly from altitudes between 90 km and 140 km. For this reasons we seek for a different mechanism, but in relation with lightning activity.

It is known that lightning are at the origin of electromagnetic emissions in the low frequency band that can result in whistlers. In case of resonance, the VLF waves interact with the electrons of the radiation belts and this interaction can modified the pitch angle of the particles, producing electron precipitation in the atmosphere [2], [3], [4], [5]. These events, also called LEP (Lightning-induced Electron Precipitations), participate to the depletion of the radiation belts. Measurements performed on board the DEMETER satellite show a whistler activity at about 2112 UT (not shown here) but, unfortunately, there are no satellite measurements during the period of observation of the HF radar echoes. At our knowledge HF radar echoes have never been related with LEP. This explanation is very preliminary and it needs further investigations but, actually, we do not have any other reasonable physical process able to explain the observation of the fast varying echoes with the properties reported in this paper.

### **Acknowledgements.**

The society Meteorage is acknowledged for providing access to their data [www.meteorage.fr](http://www.meteorage.fr). The DEMETER data were kindly provided by Hanna Rothkaehl, SRC Warsaw, Poland.

### **References**

- [1] Roussel-Dupré, R. A., and E. Blanc (1997), HF echoes from ionization potentially produced by high-altitude discharges, *J. Geophys. Res.*, 102(A3), 4613–4622.

- [2] Helliwell R. A., and S. B. Mende (1980), Correlation between  $\lambda 4278$  optical emissions and VLF wave events observed at  $L \sim 4$  in the Antarctic, *J. Geophys. Res.*, 85(A7), 3376-3386.
- [3] Chang H. C., and U. S. Inan (1985), Lightning-induced electron precipitation from the magnetosphere, *J. Geophys. Res.*, 90(A2), 1531-1541.
- [4] Carpenter D. L., and U. S. Inan (1987), Seasonal, latitudinal and diurnal distributions of whistler-induced electron precipitation events, *J. Geophys. Res.*, 92(A4), 3429-3435.
- [5] Imhof W. L., H. D. Voss, J. Mobilla, and M. Walt, Characteristics of short-duration electron precipitation bursts and their relationship with VLF wave activity, *J. Geophys. Res.*, 94(A8), 10079-10093.